Reactions of Zirconium and Hafnium Atoms with CO: Infrared Spectra and Density Functional Calculations of $M(CO)_x$, OMCCO, and $M(CO)_2^-$ (M = Zr, Hf; $x = 1-4$)

Mingfei Zhou[†] and Lester Andrews*

Contribution from the Department of Chemistry, University of Virginia, McCormick Road, Charlottesville, Virginia 22904-4319

Received October 4, 1999

Abstract: Laser-ablated zirconium and hafnium atoms were reacted with CO molecules during condensation in excess neon. The $Zr(CO)_x$ and $Hf(CO)_x$ ($x = 1-4$) carbonyls formed during sample deposition or on annealing. Ultraviolet photolysis produced the OZrCCO and OHfCCO molecules by photochemical rearrangement of the $Zr(CO)_2$ and $Hf(CO)_2$ dicarbonyls where CO is activated in the metal complex. Evidence is also presented for the $Zr(CO)_2^-$ and $Hf(CO)_2^-$ anions. The product absorptions are identified by isotopic substitutions, electron trapping with added CCl_4, and density functional theory calculations of isotopic frequencies. In contrast to the late transition metal carbonyl families, the carbonyl frequencies for TiCO, ZrCO, and HfCO decrease from 1920 to 1900 to 1869 cm^{-1} in solid neon showing an increase in $d-\pi^*$ back-bonding.

Introduction

Carbon monoxide activation and reduction by transition metal atoms are important in a great many industrial processes such as hydroformylation, alcohol synthesis, and acetic acid synthesis.[1] Coordinatively unsaturated binary transition metal carbonyls are fundamental building blocks in organometallic chemistry and are active species in catalytic reactions. Zirconium and hafnium catalysts in CO activation reactions have attracted considerable attention. A variety of zirconium and hafnium complexes have been synthesized and their reaction with carbon monoxide studied.[2−11] By contrast, the coordination chemistry of CO with zirconium and hafnium atoms is relatively sparse. Electronic states and potential energy curves of zirconium and hafnium monocarbonyls have been studied using the complete active space multi-configuration self-consistent field followed by multireference singles + doubles configuration interaction methods.[12] Ab initio calculations of zirconium monocarbonyl and dicarbonyl cations have also been reported.[13]

We have been engaged in studies of the reactions of laser-ablated metal atoms with small molecules. Recent infrared spectroscopic investigation of the reactions of laser-ablated early transition metal Nb, Ta, and actinide metal Th and U atoms with CO in this laboratory have characterized metal carbonyls as well as the inserted CMO molecules.[14−16] In addition, the photon-induced rearrangement of dicarbonyls to the OMCCO and $(\eta^2\text{-}C_2)MO_2$ isomers was observed,[14−16] which involves CO activation in a novel manner. Here we report a study of reactions of laser-ablated zirconium and hafnium atoms with CO in neon, the same photochemical rearrangement of dicarbonyls, and an interesting trend in MCO carbonyl frequencies.

Experimental and Computational Methods

The experiment for laser ablation and matrix isolation spectroscopy has been described in detail previously.[17−19] Briefly, the Nd:YAG laser fundamental (1064 nm, 10 Hz repetition rate with 10 ns pulse width) was focused on the rotating metal target (Johnson-Matthey). Laser-ablated metal atoms were co-deposited with carbon monoxide (0.05 to 0.2%) in excess neon onto a CsI cryogenic window (4K, APD Cryogenics Heliplex) at 2−4 mmol/h for 30 to 60 min using laser energies ranging from 1 to 5 mJ/pulse. Carbon monoxide (Matheson) and isotopic $^{13}C^{16}O$ and $^{12}C^{18}O$ (Cambridge Isotopic Laboratories) and selected mixtures were employed in different experiments. Infrared spectra were recorded at 0.5 cm^{-1} resolution on a Nicolet 750 spectrometer with 0.1 cm^{-1} accuracy using a HgCdTe detector. Matrix samples were annealed at different temperatures using resistance heat, and selected samples were subjected to broadband photolysis by a medium-pressure mercury arc (Philips, 175W) with the globe removed (240−580 nm).

* Address correspondence to this author. E-mail: lsa@virginia.edu.
[†] Permanent address: Laser Chemistry Institute, Fudan University, Shanghai, P. R.China.

(1) Muetterties, E. L.; Stein, *J. Chem. Rev.* **1979**, *79*, 479.
(2) Tatsumi, K.; Nakamura, A.; Hoffmann, P.; Stauffert, P.; Hoffmann, R. *J. Am. Chem. Soc.* **1985**, *107*, 4440 and references therein.
(3) Anderson, G.; Lin, M. *Organometallics*, **1988**, *7*, 2285.
(4) Curtis, C. J.; Haltiwanger, R. C. *Organometallics* **1991**, *10*, 3220.
(5) Ellis, J. E.; Frerichs, S. R.; Stein, B. K. *Organometallics* **1993**, *12*, 1048.
(6) Waldman, T. E.; Stahl, L.; Wilson, D. R. *Organometallics* **1993**, *12*, 1543.
(7) Fryzuk, M. D.; Mylvaganam, M.; MacGillivary, L. R. *Organometallics* **1996**, *15*, 1134.
(8) Erker, G.; Brackemeyer, T.; Frohlich, R. *Organometallics* **1997**, *16*, 531.
(9) Jacoby, D.; Floriani, C.; Chiesi-Villa, A. *J. Am. Chem. Soc.* **1993**, *115*, 7025.
(10) Guram, A. S.; Guo, Z. Y.; Jordan, R. T. *J. Am. Chem. Soc.* **1993**, *115*, 4902.
(11) Braunstein, P.; Cauzzi, D.; Kelly, D. *Inorg. Chem.* **1993**, *32*, 3373.
(12) Tan, H.; Liao, M. Z.; Balasubramanian, K. *J. Phys. Chem. A* **1998**, *102*, 1602.
(13) Barnes, L. A.; Rosi, M.; Bauschlicher, C. W., Jr. *J. Chem. Phys.* **1990**, *93*, 609.
(14) Zhou, M. F.; Andrews, L. *J. Phys. Chem. A*, **1999**, *103*, 7785. (NbCO).
(15) Zhou, M. F.; Andrews, L.; Li, J.; Bursten, B. E. *J. Am. Chem. Soc.* **1999**, *121*, 9712. (UCO).
(16) Zhou, M. F.; Andrews, L.; Li, J.; Bursten, B. E. *J. Am. Chem. Soc.* **1999**, *121*, 12188. (ThCO).
(17) Burkholder, T. R.; Andrews, L. *J. Chem. Phys.* **1991**, *95*, 8697.
(18) Hassanzadeh, P.; Andrews, L. *J. Phys. Chem.* **1992**, *96*, 9177.
(19) Chartihin, G. V.; Andrews, L. *J. Phys. Chem.* **1995**, *99*, 6356.

10.1021/ja9935613 CCC: $19.00
Published on Web 02/05/2000

Table 1. Infrared Absorptions (cm^{-1}) from Co-deposition of Laser-Ablated Zr Atoms with CO in Excess Neon

$^{12}C^{16}O$	$^{13}C^{16}O$	$^{12}C^{18}O$	$^{12}C^{16}O + {}^{13}C^{16}O$	*R*(12/13)	*R*(16/18)	assignment
2046.4	1985.0	2023.0	2046.4, 2037.9, 1996.0, 1985.0	1.0309	1.0116	OZrCCO
1993.1	1950.1	1944.5		1.0221	1.0250	$(Zr(CO)_6)$
1978.1	1935.0	1930.5		1.0223	1.0247	$(Zr(CO)_5)$
1971.6	1928.4	1924.6		1.0224	1.0244	$Zr_x(CO)_y$
1960.3	1915.8	1916.0	1960.2, 1948.2, 1934.1, 1916.2	1.0232	1.0231	$Zr(CO)_3$
1945.1	1903.2	1897.5		1.0220	1.0251	$(Zr(CO)_5)$
1916.6	1875.4	1869.8		1.0220	1.0250	$Zr(CO)_4$
1907.9	1866.0	1862.7		1.0225	1.0243	$Zr_x(CO)_y$
1899.5	1857.4	1855.6	1899.5, 1857.2	1.0227	1.0237	ZrCO
1898.2	1856.1	1854.7	1898.2, 1856.2	1.0227	1.0235	ZrCO site
1895.8	1853.6	1852.2	1895.6, 1853.7	1.0228	1.0235	ZrCO site
1873.4	1832.8	1828.0		1.0222	1.0248	$Zr_x(CO)_y$
1855.5	1813.4	1813.3	1855.5, 1838.3, 1813.4	1.0232	1.0233	$Zr(CO)_2$
1838.2	1798.2	1794.9	1838.3, 1820.3, 1808.5, 1797.9	1.0222	1.0241	$Zr(CO)_3$
1785.1	1746.0	1742.6	1785.1, 1761.2, 1746.0	1.0224	1.0244	$Zr(CO)_2$
1781.2	1741.2	1740.0	1781.1, 1757.0, 1755.1, 1741.4	1.0230	1.0237	$Zr_2(CO)_2$ site
1762.3	1722.9	1721.7	1762.3, 1731.3, 1722.9	1.0229	1.0236	$(Zr_2(CO)_2)$
1745.9	1706.6	1706.1	1746.0, 1731.1, 1706.5	1.0230	1.0233	$Zr(CO)_2^-$
1734.1	1696.2			1.0223		$Zr(CO)_x^-$
1682.2	1645.1		1682.1, 1652.6, 1645.2	1.0226		$Zr(CO)_2^-$
966.9	966.9	920.4	966.9	1.000	1.0505	ZrO
902.3		859.1	902.3		1.0503	OZrCCO

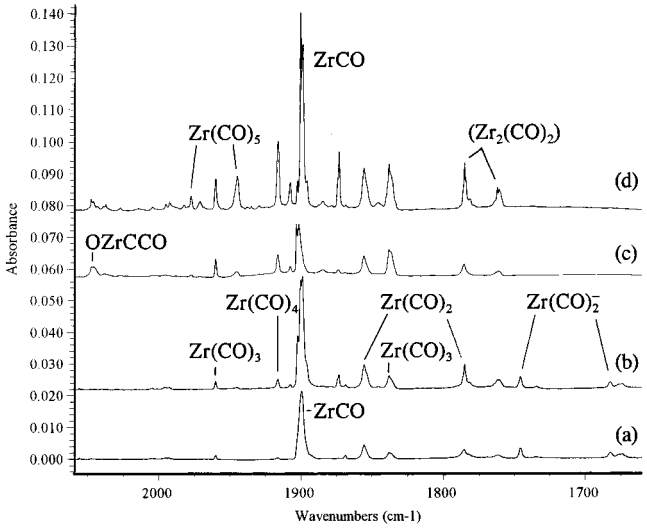

Figure 1. Infrared spectra in the 2060−1660 cm^{-1} region from co-deposition of laser ablated zirconium with 0.1%CO in neon: (a) after 30 min sample deposition at 4 K, (b) after annealing to 6 K, (c) after 15min full arc photolysis, and (d) after annealing to 8 K.

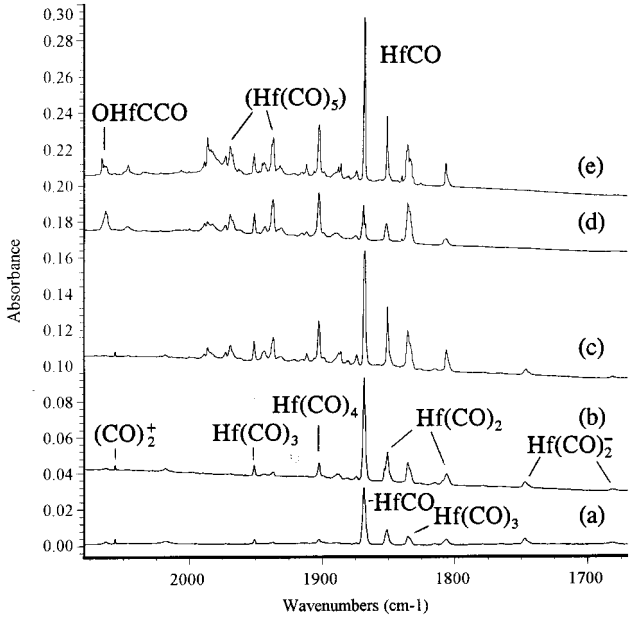

Figure 2. Infrared spectra in the 2080−1670 cm^{-1} region from co-deposition of laser ablated hafnium with 0.1% CO in neon: (a) after 30 min sample deposition at 4 K, (b) after annealing to 6 K, (c) after annealing to 8 K, (d) after 15 min full arc photolysis, and (e) after annealing to 10 K.

Density functional theoretical calculations were performed using the Gaussian 94 program.[20] Most calculations employed the BP86 functional but comparisons were done with the B3LYP functional as well.[21,22] The D95* or 6-31+G(d) basis sets for C and O atoms and the Los Alamos ECP plus DZ for Zr and Hf atoms were used.[23,24] The structures of calculated species were fully optimized and the vibrational frequencies were determined analytically with second derivatives.

Results

Infrared Spectra. The infrared spectra in the C−O stretching vibrational frequency region obtained when laser-ablated Zr and Hf atoms are co-condensed with 0.1% CO in neon are illustrated in Figures 1 and 2. The spectra reveal the strong CO absorption at 2140.7 cm^{-1}, weak absorptions for CO^+ at 2194.3 cm^{-1}, $(CO)_2^-$ at 1517.4 cm^{-1} (not shown), and $(CO)_2^+$ at 2056.3 cm^{-1},[25,26] together with absorptions due to the formation of new products, which are listed in Tables 1 and 2.

Experiments were also done with $^{13}C^{16}O$ and $^{12}C^{18}O$ samples, the same behavior was observed, and the isotopic frequencies are also listed in the tables. Similar experiments with the $^{12}C^{16}O + {}^{13}C^{16}O$ isotopic mixture gave diagnostic multiplets, which

(20) Frisch, M. J.; Trucks, G. W.; Schlegel, H. B.; Gill, P. M. W.; Johnson, B. G.; Robb, M. A.; Cheeseman, J. R.; Keith, T.; Petersson, G. A.; Montgomery, J. A.; Raghavachari, K.; Al-Laham, M. A.; Zakrzewski, V. G.; Ortiz, J. V.; Foresman, J. B.; Cioslowski, J.; Stefanov, B. B.; Nanayakkara, A.; Challacombe, M.; Peng, C. Y.; Ayala, P. Y.; Chen, W.; Wong, M. W.; Andres, J. L.; Replogle, E. S.; Gomperts, R.; Martin, R. L.; Fox, D. J.; Binkley, J. S.; Defrees, D. J.; Baker, J.; Stewart, J. P.; Head-Gordon, M.; Gonzalez, C.; Pople, J. A. *Gaussian 94, Revision B.1*; Gaussian, Inc.: Pittsburgh, PA, 1995.

(21) Perdew, J. P. *Phys. Rev. B* **1986**, *33*, 8822. Becke, A. D. *J. Chem. Phys.* **1993**, *98*, 5648.

(22) Lee, C.; Yang, E.; Parr, R. G. *Phys. Rev. B* **1988**, *37*, 785.

(23) McLean, A. D.; Chandler, G. S. *J. Chem. Phys.* **1980**, *72*, 5639. Krishnan, R.; Binkley, J. S.; Seeger, R.; Pople, J. A. *J. Chem. Phys.* **1980**, *72*, 650.

(24) Hay, P. G.; Wadt, W. R. *J. Chem. Phys.* **1985**, *82*, 299.

(25) Thompson, W. E.; Jacox, M. E. *J. Chem. Phys.* **1991**, *95*, 735.

(26) Zhou, M. F.; Andrews, L. *J. Chem. Phys.* **1999**, *110*, 10370.

Table 2. Infrared Absorptions (cm^{-1}) from Co-deposition of Laser-Ablated Hf Atoms and CO in Excess Neon

$^{12}C^{16}O$	$^{13}C^{16}O$	$^{12}C^{18}O$	$^{12}C^{16}O + {}^{13}C^{16}O$	*R*(12/13)	*R*(16/18)	assignment
2066.1	2002.9	2043.5	2066.1, 2057.1, 2013.4, 2002.9	1.0316	1.0111	OHfCCO site
2063.5	1999.9	2041.1	2063.5, 2054.2, 2011.0, 1999.9	1.0318	1.0110	OHfCCO
2046.4						$OHfCCO(CO)_x$
1986.7	1943.8	1938.3		1.0221	1.0250	$(Hf(CO)_6)$
1969.5	1926.8	1921.4		1.0222	1.0250	$(Hf(CO)_5)$
1951.2	1906.5	1907.7	1951.1, 1939.1, 1925.1, 1906.4	1.0234	1.0228	$Hf(CO)_3$
1945.3	1903.1	1898.5		1.0222	1.0247	$Hf_x(CO)_y$
1937.1	1894.7	1890.5		1.0224	1.0246	$((CO)_5)$
1911.8	1869.5	1867.0		1.0226	1.0240	$Hf_x(CO)_y$
1902.6	1861.1	1856.7		1.0223	1.0247	$Hf(CO)_4$
1885.9	1845.8	1839.5	1885.9, 1845.8	1.0217	1.0252	Hf_xCO
1874.0	1833.2	1829.0		1.0223	1.0246	$Hf_x(CO)_y$
1868.6	1826.7	1825.7	1868.5, 1826.6	1.0229	1.0235	HfCO
1850.9	1809.8	1807.6	1850.9, 1838.4, 1809.8	1.0227	1.0240	$Hf(CO)_2$
1835.5	1795.6	1793.5	1835.7, 1817.8, 1805.9, 1795.2	1.0222	1.0234	$Hf(CO)_3$
1806.7	1765.8	1765.6	1806.7, 1778.1, 1765.9	1.0232	1.0233	$Hf(CO)_2$
1747.4	1707.7	1707.9	1747.0, 1732.8, 1707.5	1.0232	1.0231	$Hf(CO)_2^-$
1681.0	1642.6		1681.7, 1656.5, 1642.6	1.0234		$Hf(CO)_2^-$
965.5		915.5		1.000	1.0546	HfO
899.9		853.2			1.0547	OHfCCO site
897.2		850.2			1.0553	OHfCCO
886.7		840.4			1.0551	$OHfCCO(CO)_x$

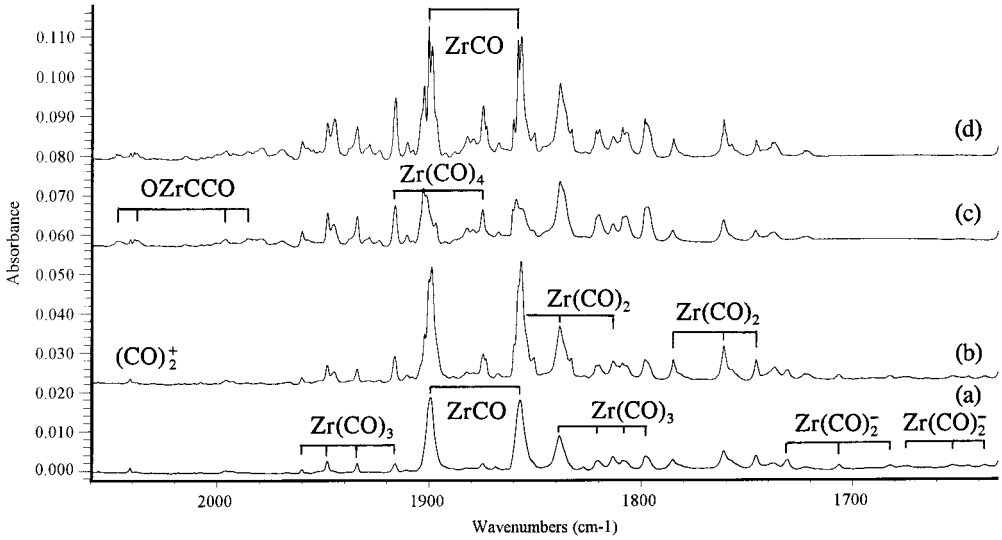

Figure 3. Infrared spectra in the 2060−1630 cm^{-1} region from co-deposition of laser ablated zirconium with 0.1% ($^{12}C^{16}O + {}^{13}C^{16}O$) in neon: (a) after 45 min sample deposition at 4 K, (b) after annealing to 8 K, (c) after 15 min full arc photolysis, and (d) after annealing to 10 K.

will be discussed below. Figures 3 and 4 show the spectra using 0.1% ($^{12}C^{16}O + {}^{13}C^{16}O$) mixed isotopic samples. Figure 5 illustrates spectra in the 980−830 cm^{-1} region for Hf, $^{12}C^{16}O$, and $^{12}C^{18}O$ in neon. In addition, experiments were done with 0.01% CCl_4 added to serve as an electron trap.[26−28] Briefly, the absorptions assigned to anions were almost eliminated from the spectra of the deposited samples on doping with CCl_4.

Calculations. DFT calculations were performed on the monocarbonyl cations, neutrals, and anions using both BP86 and B3LYP functionals and 6-31+G(d) basis sets on C and O atoms. The optimized geometries and relative energies are listed in Table 3. In general, B3LYP calculation predicted slightly longer M−C bond length and shorter C−O bond lengths and, as a result, slightly higher C−O stretching vibrational frequencies. We found the $^5\Delta$ state lowest for ZrCO and the $^3\Sigma^-$ state lowest for HfCO in agreement with post-Hartree−Fock results.[12] Table 4 lists the calculated isotopic vibrational frequencies for the structures described in Table 3 using both functionals. The CZrO and CHfO insertion products were computed to be more than 30 kcal/mol higher in energy than the monocarbonyls and are not listed here. Similar calculations were also done on dicarbonyl neutrals and anions, OMCCO isomers, and the tricarbonyls and tetracarbonyls using the BP86 functional, and the results are listed in Tables 5−8. For $Zr(CO)_{2-4}$, both D95* and 6-31+G(d) basis sets on C and O atoms were used for comparison, and the results are very similar: the calculated bond lengths are generally within 0.01 Å and C−O stretching vibrational frequencies within 10 cm^{-1}. For $Hf(CO)_{2-4}$, only the D95* basis set on C and O atoms was employed.

(27) Zhou, M. F.; Andrews, L. *J. Am. Chem. Soc.* **1998**, *120*, 11499.
(28) Zhou, M. F.; Chertihin, G. V.; Andrews, L. *J. Chem. Phys.* **1998**, *109*, 10893.

Discussion

The new product absorptions will be identified via isotopic substitutions and density functional theory calculations of isotopic frequencies.

$Hf(CO)_x$. The 1868.6 cm^{-1} band observed on sample deposition with Hf and CO increased markedly on annealing and substantially on full-arc photolysis (Figure 2). This band shifted to 1826.7 cm^{-1} with $^{13}C^{16}O$ and to 1825.7 cm^{-1} with $^{12}C^{18}O$, and gave the carbon 12/13 isotopic frequency ratio

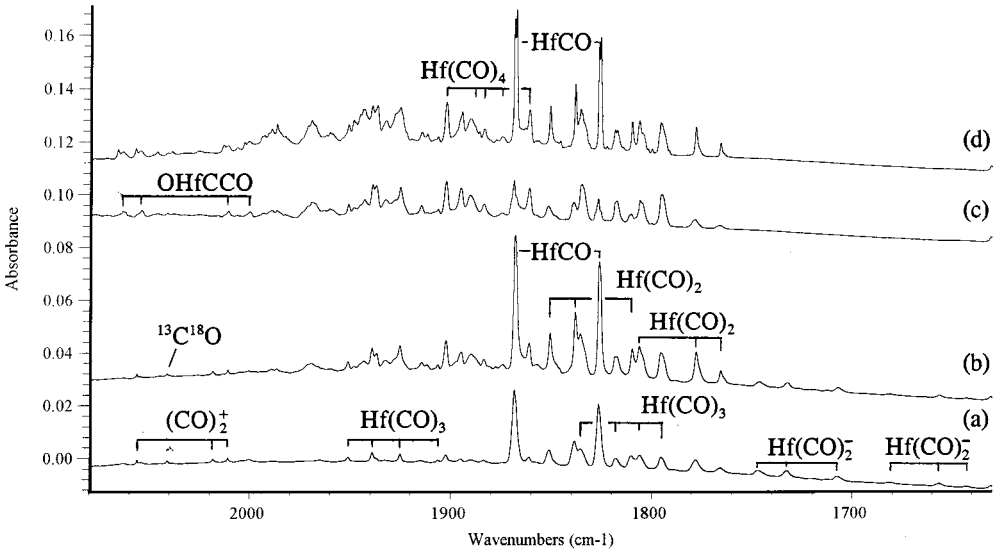

Figure 4. Infrared spectra in the 2080−1630 cm^{-1} region from co-deposition of laser ablated hafnium with 0.1% ($^{12}C^{16}O$ + $^{13}C^{16}O$) in neon: (a) after 45 min sample deposition at 4 K, (b) after annealing to 8 K, (c) after 15min full arc photolysis, and (d) after annealing to 10 K.

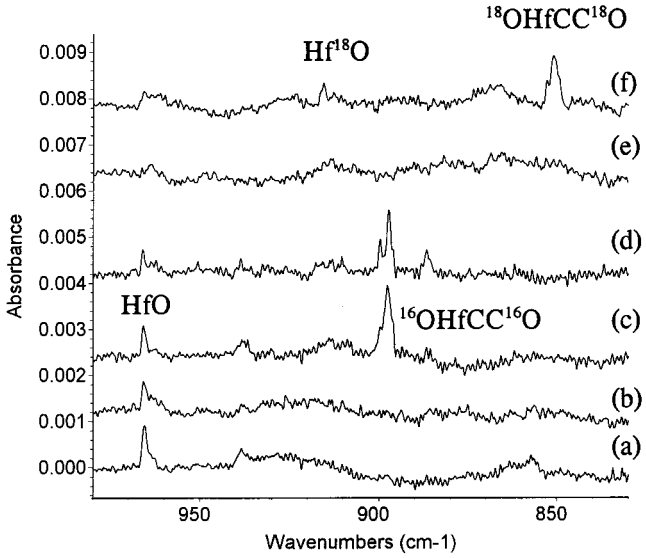

Figure 5. Infrared spectra in the 980−830 cm^{-1} region for laser-ablated hafnium co-deposited with 0.1% CO in neon (a) after 30 min deposition with $^{12}C^{16}O$, (b) after annealing to 8 K, (c) after full-arc photolysis, (d) after annealing to 10 K, (e) after 30 min deposition with $^{12}C^{18}O$, and (f) after full-arc photolysis.

1.0229 and the oxygen 16/18 isotopic frequency ratio 1.0235. In the mixed $^{12}C^{16}O$ + $^{13}C^{16}O$ spectra, only pure isotopic counterparts were presented, which confirms that only one CO submolecule is involved in this vibrational mode. This band is the major product absorption on sample deposition with laser energy ranging from 1 to 5 mJ/pulse, which suggests a single Hf atom species. The 1868.6 cm^{-1} band is assigned to the C−O stretching vibration of the HfCO molecule. Our DFT calculations predict the HfCO molecule to have a $^3\Sigma^-$ ground state with C−O stretching vibrational frequency at 1864.3 cm^{-1} using BP86 and at 1929.7 cm^{-1} using B3LYP with calculated isotopic frequency ratios (Table 4) in excellent agreement as B3LYP frequencies are typically higher than observed values.[26,28] The earlier CASMCSCF and MRSDCI calculations also found a $^3\Sigma^-$ ground state for HfCO and gave a much higher C−O stretching frequency (2149 and 2153 cm^{-1}),[12] because not enough C and O orbitals are included in the active space to accurately describe the C−O stretch.

Table 3. Geometries and Relative Energies (kcal/mol) Calculated for MCO, MCO$^-$, and MCO$^+$ [a]

	molecule	state	rel energy	M−C (Å)	C−O (Å)
BP86	ZrCO	$^5\Delta(\sigma^1\pi^2\delta^1)^b$	0	2.132	1.184
		$^3\Sigma^-(\sigma^2\pi^2)^c$	+5.7	2.109	1.183
	$ZrCO^-$	$^4\Delta(\sigma^2\pi^2\delta^1)$	−22.9	2.135	1.204
	$ZrCO^+$	$^4\Delta(\pi^2\delta^1)$	+156.3	2.160	1.164
	HfCO	$^3\Sigma^-(\sigma^2\pi^2)^d$	0	2.070	1.186
		$^5\Delta(\sigma^1\pi^2\delta^1)^b$	+11.5	2.089	1.190
	$HfCO^-$	$^4\Delta(\sigma^2\pi^2\delta^1)$	−21.0	2.117	1.213
		$^2\Pi(\sigma^2\pi^3)$	−22.6	2.017	1.232
	$HfCO^+$	$^4\Sigma^-(\sigma^1\pi^2)$	+168.2	2.077	1.164
		$^2\Pi(\sigma^2\pi^1)$	+177.8	2.066	1.167
B3LYP	ZrCO	$^5\Delta(\sigma^1\pi^2\delta^1)$	0	2.147	1.170
		$^3\Sigma^-(\sigma^2\pi^2)$	+4.4	2.122	1.167
	$ZrCO^-$	$^4\Delta(\sigma^2\pi^2\delta^1)$	−22.3	2.141	1.192
	$ZrCO^+$	$^4\Delta(\pi^2\delta^1)$	+149.9	2.197	1.147
	HfCO	$^3\Sigma^-(\sigma^1\pi^2)$	0	2.077	1.172
		$^5\Delta(\sigma^1\pi^2\delta^1)$	+16.0	2.093	1.178
	$HfCO^-$	$^4\Delta(\sigma^2\pi^2\delta^1)$	−17.4	2.116	1.203
		$^2\Pi(\sigma^2\pi^3)$	−17.8	2.018	1.219
	$HfCO^+$	$^4\Sigma^-(\sigma^1\pi^2)$	+167.3	2.100	1.149
		$^2\Pi(\sigma^2\pi^1)$	+173.4	2.227	1.136

[a] 6-31+G(d) basis set on C and O atoms. [b] $\langle S^2\rangle$ is 6.0011 before annihilation and 6.0000 after. [c] $\langle S^2\rangle$ is 2.7562 before annihilation and 2.0013 after. [d] $\langle S^2\rangle$ is 2.0529 before annihilation and 2.001 after.

Major growth in the HfCO absorption on 6 K annealing (Figure 2) is in accord with direct reaction of ground-state Hf (^{3}F) atoms[29] with CO, reaction 1, to give HfCO ($^3\Sigma^-$) in the neon matrix.

$$Hf(^3F) + CO(^1\Sigma^+) \rightarrow HfCO(^3\Sigma^-) \quad (1)$$

The 1850.9 and 1806.7 cm^{-1} bands were weakly observed on sample deposition, they increased together markedly on annealing, but greatly decreased on photolysis. Both bands exhibited characteristic carbonyl C−O stretching vibrational frequency ratios as listed in Table 2. In the $^{12}C^{16}O$ + $^{13}C^{16}O$ mixed isotopic experiment, triplet absorptions with approximately 1:2:1 relative intensities were observed (Figure 4), which demonstrates that two equivalent CO submolecules are involved in these modes. Accordingly, these two bands are assigned to the symmetric and antisymmetric C−O stretching vibrations of

(29) Moore, C. E. *Atomic Energy Levels*; National Bureau of Standards Publication 467; National Bureau of Standards: Washington, DC, 1958.

Table 4. Isotopic Frequencies (cm^{-1}), Intensities (km/mol), and Isotopic Frequency Ratios Calculated for the Structures Described in Table 3

	molecule	$^{12}C^{16}O$	$^{12}C^{16}O$	$^{12}C^{16}O$	*R*(12/13)	*R*(16/18)
BP86	ZrCO	1873.9(880)	1830.9(835)	1830.6(847)	1.0235	1.0237
	$^5\Delta$	403.9(6)	398.8(6)	393.1(5)	1.0128	1.0275
		285.0(3×2)	276.5(3)	281.3(4)	1.0307	1.0132
	$^3\Sigma^-$	1877.4(883)	1834.2(839)	1834.2(848)	1.0236	1.0236
		415.4(3)	410.2(3)	404.2(3)	1.0127	1.0277
		304.2(2)[a]	295.1(2)	300.2(2)	1.0308	1.0133
		295.1(2)	286.3(2)	291.3(2)	1.0307	1.0130
	$ZrCO^-$	1767.1(961)	1725.9(920)	1727.2(915)	1.0239	1.0231
	$^4\Delta$	406.2(0.2)	401.2(0.3)	395.1(0.2)	1.0125	1.0281
		283.9(5×2)	275.5(5)	280.3(5)	1.0305	1.0128
	$ZrCO^+$	1988.2(515)	1943.2(487)	1941.3(498)	1.0232	1.0242
	$^4\Delta$	380.3(3)	375.4(3)	370.3(2)	1.0131	1.0270
		289.6(7×2)	281.1(6)	285.8(7)	1.0302	1.0133
	HfCO	1864.3(716)	1821.3(679)	1821.5(690)	1.0236	1.0235
	$^3\Sigma^-$	407.6(6)	401.8(6)	395.2(5)	1.0144	1.0314
		304.2(0)[a]	295.2(0)	300.3(0)	1.0305	1.0130
		303.2(0)	294.2(0)	299.3(0)	1.0305	1.0130
	$^5\Delta$	1846.6(786)	1803.7(747)	1804.7(754)	1.0238	1.0232
		406.9(2)	401.2(2)	394.4(2)	1.0142	1.0317
		296.0(4×2)	287.2(3)	292.2(4)	1.0306	1.0130
	$HfCO^-$	1725.3(865)	1684.7(833)	1686.8(815)	1.0241	1.0228
	$^4\Delta$	389.2(9)	383.8(8)	377.0(8)	1.0141	1.0324
		278.8(0×2)	270.5(0)	275.3(0)	1.0307	1.0127
	$^2\Pi$	1628.3(940)	1589.5(901)	1592.9(893)	1.0244	1.0222
		452.4(2)	446.3(1)	438.1(2)	1.0137	1.0326
		335.0(19)[b]	324.9(17)	330.8(20)	1.0311	1.0127
		309.1(1)	299.8(1)	305.2(1)	1.0310	1.0128
	$HfCO^+$	1983.3(506)	1938.2(475)	1936.8(493)	1.0233	1.0240
	$^4\Delta$	396.1(14)	390.3(13)	384.2(12)	1.0149	1.0310
		321.2(1×2)	311.6(1)	317.0(1)	1.0308	1.0132
B3LYP	ZrCO	1942.0(1260)	1898.1(1194)	1896.2(1216)	1.0231	1.0242
	$^5\Delta$	391.2(17)	386.2(17)	380.9(15)	1.0129	1.0270
		288.1(2×2)	279.6(1)	284.3(2)	1.0304	1.0134
	$^3\Sigma^-$	1952.0(1332)	1907.8(1263)	1906.1(1283)	1.0232	1.0241
		402.1(12)	396.9(13)	391.4(11)	1.0131	1.0273
		302.1(1)[a]	293.2(1)	298.2(1)	1.0304	1.0131
		284.2(0.1)	275.8(0.1)	280.5(0.1)	1.0305	1.0132
	$ZrCO^+$	2092.6(705)	2045.8(665)	2042.4(683)	1.0229	1.0246
	$^4\Delta$	351.4(9)	346.8(8)	342.3(8)	1.0133	1.0266
		289.5(5×2)	281.0(5)	285.6(5)	1.0302	1.0137
	$ZrCO^-$	1815.6(1281)	1773.8(1223)	1773.9(1222)	1.0236	1.0235
	$^4\Delta$	404.9(2)	399.8(2)	394.0(2)	1.0128	1.0277
		288.8(5×2)	280.2(5)	285.0(5)	1.0307	1.0133
	HfCO	1929.7(1007)	1885.8(954)	1884.5(973)	1.0233	1.0240
	$^3\Sigma^-$	400.8(13)	394.9(13)	388.7(12)	1.0149	1.0311
		311.7(0×2)	302.5(0)	307.7(0)	1.0304	1.0130
	$^5\Delta$	1901.5(1083)	1857.9(1028)	1857.6(1042)	1.0235	1.0236
		406.5(5)	400.6(5)	394.2(5)	1.0147	1.0312
		301.7(3×2)	292.7(3)	297.8(3)	1.0307	1.0131
	$HfCO^+$	2075.1(721)	2028.5(677)	2025.5(703)	1.0230	1.0245
	$^4\Sigma^-$	372.6(26)	367.0(25)	361.5(23)	1.0153	1.0307
		321.1(0.2×2)	314.5(0.2)	319.8(0.2)	1.0210	1.0041
	$HfCO^-$	1673.2(1238)	1633.9(1185)	1635.9(1177)	1.0241	1.0228
	$^2\Pi$	454.0(1)	447.7(1)	439.8(1)	1.0141	1.0323
		340.4(23)[b]	330.2(21)	336.1(24)	1.0309	1.0128
		318.6(2)	309.0(2)	314.5(2)	1.0311	1.0130
	$HfCO^-$	1766.9(1103)	1725.7(1060)	1727.0(1041)	1.0239	1.0231
	$^4\Delta$	394.8(7)	389.3(7)	382.6(7)	1.0141	1.0319
		287.3(0×2)	278.7(0)	283.6(0)	1.0309	1.0130

[a] Degenerate bending mode split owing to spin contamination from quintet state. [b] Degenerate π_x and π_y bending modes split by calculation.

the bent $Hf(CO)_2$ molecule. Our DFT calculation predicted a $^3B_2$ ground state for the $Hf(CO)_2$ molecule with an C−Hf−C bond angle of 96.6°, and the antisymmetric and symmetric C−O stretching vibrational frequencies were calculated (BP86) at 1828.2 and 1822.6 cm^{-1}, respectively. The calculated frequencies are in ±1% agreement with our observed values.

$$HfCO(^3\Sigma^-) + CO(^1\Sigma^+) \rightarrow Hf(CO)_2(^3B_2) \qquad (2)$$

The 1835.5 and 1951.2 cm^{-1} bands increased together on annealing, suggesting two different modes of the same molecule. The lower band shifted to 1795.6 cm^{-1} with $^{13}C^{16}O$ and to 1793.5 cm^{-1} with $^{12}C^{18}O$, which defines the 12/13 ratio 1.0222 and the 16/18 ratio 1.0234. In the mixed $^{12}C^{16}O + {}^{13}C^{16}O$ experiment, a quartet at 1835.7, 1817.8, 1805.9, and 1795.2 cm^{-1} with approximately 3:1:1:3 relative intensities was observed; this quartet mixed isotopic structure is characteristic of the doubly degenerate mode of a trigonal species.[30] In concert, the upper band shifted to 1906.5 cm^{-1} with $^{13}C^{16}O$ and to 1907.7

(30) Darling, J. H.; Ogden, J. S. *J. Chem. Soc., Dalton Trans.* **1972**, 2496.

Table 5. Geometries and Relative Energies (kcal/mol) Calculated for $M(CO)_2$, $M(CO)_2^-$, and OMCCO Molecules Using the BP86 Functional

molecule	state	rel energy	geometry[e]
$Zr(CO)_2$[a]	$^5B_2$	0	Zr−C, 2.164; C−O, 1.182; ∠CZrC, 88.1; ∠ZrCO, 179.5
	$^3B_2$	+0.8	Zr−C, 2.094; C−O, 1.193; ∠CZrC, 79.2; ∠ZrCO, 177.6
OZrCCO[a]	$^1A'$	−33.9	O−Zr, 1.776; Zr−C, 2.005; C−C, 1.322; C−O, 1.198; ∠OZrC, 108.3
$Zr(CO)_2^-$ [a]	$^4B_2$	−35.3	Zr−C, 2.106; C−O, 1.211; ∠CZrC, 83.0; ∠ZrCO, 178.9
	$^2B_2$	−28.2	Zr−C, 2.100; C−O, 1.211; ∠CZrC, 80.8; ∠ZrCO, 178.2
$Zr(CO)_2$[b]	$^5B_2$	0	Zr−C, 2.167; C−O, 1.177; ∠CZrC, 87.7; ∠ZrCO, 179.5
	$^3B_2$	+0.8	Zr−C, 2.096; C−O, 1.188; ∠CZrC, 79.8; ∠ZrCO, 177.9
OZrCCO [b,c]	$^1A'$	−32.1	O−Zr, 1.784; Zr−C, 2.002; C−C, 1.315; C−O, 1.195; ∠OZrC, 108.4
$Zr(CO)_2^-$ [b]	$^4B_2$	−38.1	Zr−C, 2.106; C−O, 1.207; ∠CZrC, 83.3; ∠ZrCO, 178.9
	$^2B_2$	−31.1	Zr−C, 2.101; C−O, 1.207; ∠CZrC, 82.0; ∠ZrCO, 178.6
$Hf(CO)_2$[b]	$^3B_2$	0	Hf−C, 2.091; C−O, 1.191; ∠CHfC, 96.6; ∠HfCO, 179.7
	$^1A_1$	+2.5	Hf−C, 2.102; C−O, 1.188; ∠CHfC, 132.5; ∠HfCO, 177.3
$Hf(CO)_2$- [a]	$^4B_2$	−48.2	Hf−C, 2.090; C−O, 1.212; ∠CHfC, 78.8; ∠HfCO, 179.0
OHfCCO[a,d]	$^1A'$	−48.3	O−Hf, 1.761; Hf−C, 1.987; C−C, 1.320; C−O, 1.197; ∠OHfC, 108.7

[a] D95* basis set on C and O atoms. [b] 6-31+G(d) basis set on C and O atoms. [c] For comparison, a similar calculation for ZrO yielded a $^1\Sigma^+$ state, 1.750 Å bond length, and 970.0 cm^{-1} harmonic frequency, and 128 km/mol intensity. [d] For comparison, a similar calculation for HfO yielded a $^1\Sigma^+$ state, 1.734 Å bond length, 968.0 cm^{-1}, 95 km/mol. [e] Distances in Å and angles in deg.

Table 6. Calculated Isotopic Frequencies (cm^{-1}), Intensities (km/mol), and Isotopic Frequency Ratios for the Structures Described in Table 5

molecule	$(^{12}C^{16}O)_2$	$(^{13}C^{16}O)_2$	$(^{12}C^{18}O)_2$	*R*(12/13)	*R*(16/18)
$Zr(CO)_2$[a]	1877.4(1048)(b_2)	1834.7(993)	1833.6(1009)	1.0233	1.0239
($^5B_2$)	1922.2(728)(a_1)	1878.0(691)	1877.9(699)	1.0235	1.0236
$Zr(CO)_2$[a]	1814.5(856)(b_2)	1772.7(814)	1773.0(822)	1.0236	1.0234
($^3B_2$)	1836.3(1275)(a_1)	1794.5(1205)	1793.5(1234)	1.0233	1.0239
OZrCCO[a]	902.7(181)(a′)	902.6(182)	859.1(165)	1.0001	1.0508
($^1A'$)	1320.6(19)(a′)	1284.7(21)	1297.3(16)	1.0279	1.0180
	2076.7(1267)(a′)	2012.3(1186)	2053.5(1241)	1.0320	1.0113
$Zr(CO)_2^-$ [a]	1719.8(919)(b_2)	1679.7(877)	1681.0(878)	1.0239	1.0231
($^4B_2$)	1767.1(1244)(a_1)	1725.9(1187)	1727.4(1189)	1.0239	1.0230
$Zr(CO)_2^-$ [a]	1719.8(785)(b_2)	1679.6(749)	1681.2(750)	1.0239	1.0230
($^2B_2$)	1760.2(1516)(a_1)	1719.2(1445)	1720.5(1451)	1.0238	1.0231
$Zr(CO)_2$[b]	1883.7(1132)(b_2)	1840.9(1073)	1839.6(1091)	1.0232	1.0240
($^5B_2$)	1930.3(756)(a_1)	1886.0(718)	1885.7(727)	1.0235	1.0237
$Zr(CO)_2$[b]	1815.5(993)(b_2)	1773.8(943)	1773.7(953)	1.0235	1.0236
($^3B_2$)	1841.3(1296)(a_1)	1799.4(1225)	1798.2(1253)	1.0233	1.0240
OZrCCO[b]	891.1(210)(a′)	891.0(211)	848.0(191)	1.0001	1.0508
($^1A'$)	1341.2(17)(a′)	1305.1(19)	1317.0(14)	1.0277	1.0184
	2072.5(1370)(a′)	2007.5(1284)	2050.3(1342)	1.0324	1.0108
$Zr(CO)_2^-$ [b]	1712.7(1123)(b_2)	1672.9(1071)	1673.9(1074)	1.0238	1.0232
($^4B_2$)	1765.1(1385)(a_1)	1724.1(1322)	1725.2(1323)	1.0238	1.0231
$Zr(CO)_2^-$ [b]	1714.0(978)(b_2)	1674.1(932)	1675.2(935)	1.0238	1.0232
($^2B_2$)	1761.4(1621)(a_1)	1720.5(1546)	1721.6(1549)	1.0238	1.0231
$Hf(CO)_2$[a]	1828.2(1146)(b_2)	1786.1(1089)	1786.2(1100)	1.0236	1.0235
($^3B_2$)	1822.6(1584)(a_1)	1781.7(1488)	1779.1(1547)	1.0230	1.0245
$Hf(CO)_2$[a]	1828.4(2094)(b_2)	1787.3(1984)	1784.9(2020)	1.0230	1.0244
($^1A_1$)	1890.1(423)(a_1)	1846.2(399)	1847.2(411)	1.0238	1.0232
OHfCCO[a]	888.3(140)(a′)	888.2(140)	841.7(125)	1.0001	1.0554
($^1A'$)	1334.2(4)(a′)	1297.9(5)	1310.5(3)	1.0280	1.0181
	2088.2(1393)(a′)	2023.1(1307)	2065.3(1363)	1.0322	1.0111
$Hf(CO)_2^-$ [a]	1727.5(769)(b_2)	1686.8(736)	1689.2(732)	1.0241	1.0227
($^4B_2$)	1751.5(1689)(a_1)	1710.9(1605)	1711.6(1623)	1.0237	1.0233

[a] D95* basis set on C and O atoms. [b] 6-31+G(d) basis set on C and O atoms.

Table 7. Calculated C−O Stretching Vibrational Frequencies (cm^{-1}), Intensities (km/mol), and Isotopic Frequency Ratios for $Zr(CO)_3$ and $Hf(CO)_3$ Molecules Using BP86 Density Functional

molecule	$(^{12}C^{16}O)_3$	$(^{12}C^{16}O)_3$	$(^{12}C^{16}O)_3$	*R*(12/13)	*R*(16/18)
$Zr(CO)_3$[a]	1847.7(998×2)(e)	1805.8(947)	1804.3(961)	1.0232	1.0241
($^3A_1$)	1932.8(400)(a_1)	1887.8(381)	1889.0(382)	1.0238	1.0232
$Zr(CO)_3$[b]	1850.8(1124×2)(e)	1809.0(1066)	1807.1(1083)	1.0231	1.0242
($^3A_1$)	1941.8(402)(a_1)	1896.7(383)	1897.7(384)	1.0238	1.0232
$Hf(CO)_3$[c]	1846.7(906×2)(e)	1804.1(860)	1804.2(872)	1.0236	1.0236
($^3A_1$)	1915.4(590)(a_1)	1870.8(560)	1872.2(568)	1.0238	1.0231

[a] D95* basis set on C and O atoms, structure, C_{3v} symmetry, Zr−C 2.127 Å, C−O 1.185 Å, ∠CZrC 80.5°, ∠ZrCO 177.8°. [b] 6-31+G(d) basis set on C and O atoms, structure, C_{3v} symmetry, Zr−C 2.131 Å, C−O 1.180 Å, ∠CZrC 80.6°, ∠ZrCO 177.8°. [c] D95* basis set on C and O atoms, structure, C_{3v} symmetry, Hf−C 2.089 Å, C−O 1.187 Å, ∠CHfC 79.0°, ∠HfCO 179.6°.

cm^{-1} with $^{12}C^{18}O$, and showed slightly more C and less O involvement than the lower band. In the mixed $^{12}C^{16}O + {}^{13}C^{16}O$ experiments, a quartet at 1951.1, 1939.1, 1925.1, and 1906.4 cm^{-1} with approximately 1:3:3:1 relative intensities was observed, which demonstrates the nondegenerate vibrational mode of a trigonal species. These two bands are assigned to the antisymmetric (e_1) and symmetric (a_1) C−O stretching vibrations, respectively, of the $Hf(CO)_3$ molecule with C_{3v} symmetry.

Table 8. Calculated C−O Stretching Vibrational Frequencies (cm^{-1}), Intensities (km/mol), and Isotopic Frequency Ratios for $Zr(CO)_4$ and $Hf(CO)_4$ Molecules Using BP86 Density Functional

molecule	$(^{12}C^{16}O)_4$	$(^{12}C^{16}O)_4$	$(^{12}C^{16}O)_4$	*R*(12/13)	*R*(16/18)
$Zr(CO)_4$[a]	1887.4(1862×3)(t_2)	1845.2(1762)	1842.1(1799)	1.0229	1.0246
($^1A_1$)	1987.6(0)(a_1)	1941.4(0)	1942.4(0)	1.0238	1.0233
$Zr(CO)_4$[b]	1896.0(1993×3)(t_2)	1853.8(1886)	1850.4(1926)	1.0228	1.0246
($^1A_1$)	1998.1(0)(a_1)	1951.9(0)	1952.5(0)	1.0237	1.0234
$Hf(CO)_4$[c]	1880.0(1862×3)(t_2)	1837.7(1762)	1835.4(1799)	1.0230	1.0243
($^1A_1$)	1986.1(0)(a_1)	1939.5(0)	1941.7(0)	1.0240	1.0229

[a] D95* basis set on C and O atoms, structure, T_d symmetry, Zr−C 2.204 Å, C−O 1.178 Å. [b] 6-31+G(d) basis set on C and O atoms, structure, T_d symmetry, Zr−C 2.210 Å, C−O 1.173 Å. [c] D95* basis set on C and O atoms, structure, T_d symmetry, Hf−C 2.162 Å, C−O 1.180 Å.

The assignments are further confirmed by DFT/BP86 calculations, which predicted a $^3A_1$ ground state for the $Hf(CO)_3$ molecule in C_{3v} symmetry; the antisymmetric and symmetric C−O stretching vibrations were calculated at 1846.7 and 1915.4 cm^{-1} with 906×2 and 590 relative intensities in reasonable agreement with the observations.

$$Hf(CO)_2(^3B_2) + CO(^1\Sigma^+) \rightarrow Hf(CO)_3(^3A_1) \qquad (3)$$

The 1902.6 cm^{-1} absorption only appeared on annealing after the $Hf(CO)_{1-3}$ absorptions, increased markedly on 8 K annealing, and shifted to 1861.1 cm^{-1} in $^{13}C^{16}O$ and to 1856.7 cm^{-1} in $^{12}C^{18}O$ spectra. As shown in Figure 4, a quintet was observed in the mixed $^{12}C^{16}O + {}^{13}C^{16}O$ experiment, which is the characteristic feature for the triply degenerate mode of a tetrahedral species.[30] On this evidence the 1902.6 cm^{-1} band is assigned to the antisymmetric C−O stretching vibration of the $Hf(CO)_4$ molecule with T_d symmetry. Our BP86 calculation predicts a $^1A_1$ ground state for $Hf(CO)_4$ with T_d symmetry and a strong antisymmetric C−O stretching vibration at 1880.0 cm^{-1}, just under the observed value. As listed in Table 8, the calculated isotopic frequency ratios are also in accord with observed experimental values. Apparently spin conservation is less important for reaction to form the higher carbonyls in the matrix.[28]

$$Hf(CO)_3(^3A_1) + CO(^1\Sigma^+) \rightarrow Hf(CO)_4(^1A_1) \qquad (4)$$

Absorptions at 1937.1, 1969.5, and 1986.7 cm^{-1} increase markedly on higher temperature annealing and show carbonyl C−O stretching vibrational frequency ratios, but the mixed isotopic structure cannot be resolved. The 1931.7 and 1969.5 cm^{-1} bands track together and are tentatively assigned to the $Hf(CO)_5$ molecule, and the 1986.7 cm^{-1} band to the $Hf(CO)_6$ molecule.

$Zr(CO)_x$. The 1899.5 cm^{-1} band is the major product absorption on sample deposition with Zr in both lower and higher CO concentration experiments; it increased on annealing and greatly decreased on photolysis. In the mixed $^{12}C^{16}O + {}^{13}C^{16}O$ isotopic experiment, a doublet at 1899.5 and 1857.2 cm^{-1} was observed, which indicates that one CO subunit is involved in this mode. The 1899.5 cm^{-1} band is assigned to the C−O stretching vibration of the ZrCO molecule. Recent high-level CASMCSCF calculations found two nearly degenerate electronic states ($^5\Delta$, $^3\Sigma^-$) as candidates for the ground state of ZrCO.[12] The $^3\Sigma^-$ state is derived primarily from the ^3F atomic Zr ground state, and the $^5\Delta$ state correlates mainly with the ^5F atomic Zr state, which is about 13643 cm^{-1} above the ground state.[29] The present BP86 and B3LYP calculations both predict the lowest state to be $^5\Delta$, with the $^3\Sigma^-$ state slightly higher in energy (5.7 kcal/mol by BP86 and 4.4 kcal/mol by B3LYP). As listed in Table 4, the calculated C−O stretching vibrational frequencies for these two state are very close: 1873.9 cm^{-1} with BP86 and 1942.0 cm^{-1} with B3LYP for the $^5\Delta$ state, and at 1877.4 cm^{-1} with BP86 and 1952.0 cm^{-1} with B3LYP for the $^3\Sigma^-$ state. Of equal importance, the calculated C−O stretching vibrational frequency ratios are essentially the same for both states, which makes it difficult to determine experimentally which state is the ground state. However, the ZrCO absorption increases 2-fold on 6 K annealing (Figure 1), indicating that ground state Zr reacts with CO, which strongly suggests that the ground state of ZrCO is $^3\Sigma^-$. Higher level CASMCSCF and MRSDCI calculations[12] predict the C−O stretching vibrational frequency too high (2132, 2143 cm^{-1} for $^5\Delta$ and 2129, 2133 cm^{-1} for $^3\Sigma^-$) to be of diagnostic value owing to the lack of sufficient C and O orbitals in the active space to accurately describe the C−O stretching mode.

The 1855.5 cm^{-1} band increased on annealing after the ZrCO absorption. It shifted to 1813.4 and to 1813.3 cm^{-1} using $^{13}C^{16}O$ and $^{12}C^{18}O$ samples, which define the 12/13 ratio 1.0232 and the 16/18 ratio 1.0233. This band is assigned to the symmetric C−O stretching vibration of the bent $Zr(CO)_2$ molecule based on triplet isotopic structure in the mixed $^{12}C^{16}O + {}^{13}C^{16}O$ experiment. A 1785.1 cm^{-1} band also increased on annealing and exhibited slightly less carbon isotopic shift and more oxygen isotopic shift. In the mixed $^{12}C^{16}O + {}^{13}C^{16}O$ experiment, a triplet is observed, and this band is assigned to the antisymmetric C−O stretching vibration of the $Zr(CO)_2$ molecule. The present DFT calculations predicted $^5B_2$ and $^3B_2$ states very close in energy. The antisymmetric and symmetric vibrational frequencies were calculated at 1877.4 and 1922.2 cm^{-1} for the $^5B_2$ state, and at 1814.5 and 1836.3 cm^{-1} for the $^3B_2$ state using the 6-31+G(d) basis set on C and O atoms. The $^3B_2$ state frequencies fit better and suggest that the ground state of $Zr(CO)_2$ is the $^3B_2$ state.

Sharp bands at 1960.3 and 1838.2 cm^{-1} increased together on annealing. In the mixed $^{12}C^{16}O + {}^{13}C^{16}O$ experiment, a quartet with approximately 1:3:3:1 relative intensities was observed for the upper band, while a quartet with approximately 3:1:1:3 relative intensities was produced for the lower band, which are characteristic of nondegenerate and degenerate modes of a trigonal species.[30] These two bands are assigned to the $Zr(CO)_3$ molecule with C_{3v} symmetry following the $Hf(CO)_3$ assignment. Our BP86 calculation predicted the $Zr(CO)_3$ molecule to have a $^3A_1$ ground state with symmetric and antisymmetric C−O stretching vibrations at 1941.8 and 1850.8 cm^{-1} with 402:1124×2 relative intensities using the 6-31+G(d) basis set on C and O atoms, which is excellent agreement.

The 1916.6 cm^{-1} band appeared on annealing after the $Zr(CO)_{1-3}$ absorptions and is assigned to the $Zr(CO)_4$ molecule, which was calculated to have a $^1A_1$ ground state with T_d symmetry and a strong triply degenerate C−O stretching vibrational frequency at 1896.0 cm^{-1}.

The 1945.1, 1978.1, and 1993.1 cm^{-1} bands increased markedly on higher temperature annealing, and are due to higher carbonyl species; unfortunately, the mixed isotopic structure could not be resolved. The 1945.1 and 1978.1 cm^{-1} absorptions

go together and are tentatively assigned to the $Zr(CO)_5$ molecule, and the 1993.1 cm^{-1} band to the $Zr(CO)_6$ molecule.

OMCCO. The 2063.5 and 897.2 cm^{-1} bands appeared in the Hf + CO experiments only on photolysis, and these bands sharpened and decreased together on further annealing. Photolysis using $\lambda > 380$ nm gave 20% of the 2063.5 cm^{-1} band absorbance and $\lambda > 290$ nm irradiation gave almost as much as the full arc. The 2063.5 cm^{-1} band shifted to 1999.9 cm^{-1} with $^{13}C^{16}O$ sample and to 2041.1 cm^{-1} with $^{12}C^{18}O$ sample, which defined a much larger 12/13 ratio (1.0318) and smaller 16/18 ratio (1.0110) compared with harmonic diatomic C−O ratios. In the mixed $^{12}C^{16}O + {}^{13}C^{16}O$ experiment, a quartet at 2063.5, 2054.2, 2011.0, and 1999.9 cm^{-1} with approximately 1:1:1:1 relative intensities was produced, which indicates that two inequivalent C atoms are involved in this vibrational mode (Figure 4). The 897.2 cm^{-1} band showed no carbon isotopic effect, but shifted to 850.2 cm^{-1} in $^{12}C^{18}O$ spectra (Figure 5). The isotopic 16/18 ratio 1.0553 is just under the harmonic diatomic HfO ratio (1.0554), which indicates that this band is due to a terminal Hf−O stretching vibration. These two bands are assigned to the antisymmetric C−C−O and Hf−O stretching vibrations of the OHfCCO molecule following the ONbCCO, OTaCCO, OThCCO, and OUCCO examples.[14−16]

The present BP86 calculations predict a $^1A'$ ground-state OHfCCO with bent (O−Hf−C angle 108.7°) geometry, which is 48.3 kcal/mol more stable than the $^3B_2$ $Hf(CO)_2$ dicarbonyl molecule. The C−O and Hf−O stretching vibrations are calculated to be 2088.2 and 888.3 cm^{-1}, which require 0.988 and 1.010 scale factors to match the experimental values. Of more importance, the calculated isotopic ratios (12/13:1.0322, 1.0001, and 16/18:1.0111, 1.0554) are almost the same as the observed values (Table 2). The symmetric C−C−O stretching vibration, predicted at 1334.2 cm^{-1} with only 0.3% of the antisymmetric stretching mode intensity, cannot be observed. As a calibration, the same calculation for HfO gave a 968.0 cm^{-1} frequency with a 965.5 observed/968.0 calculated = 0.997 scale factor.

Similar bands produced on ultraviolet photolysis at 2046.4 and 902.3 cm^{-1} in the Zr + CO experiments are assigned to the OZrCCO molecule. A previous photolysis with $\lambda > 380$ nm gave about 10% of the 2046.4 cm^{-1} product absorbance shown in Figure 1. Our DFT calculation predicts the OZrCCO molecule to have a $^1A'$ ground state, which is 33.9 kcal/mol lower in energy than the $Zr(CO)_2$ molecule. The C−O and Zr−O stretching vibrations were calculated at 2072.5 and 891.1 cm^{-1} and the calculated isotopic frequency ratios (Table 6) are in excellent agreement with observed values. The ZrO diatomic was calculated to have a 970.0 cm^{-1} fundamental, 3.1 cm^{-1} above the neon matrix value observed here.

The OHfCCO and OZrCCO absorptions are *produced* on photolysis when the $Hf(CO)_2$ and $Zr(CO)_2$ absorptions *decreased*, suggesting that they are formed by activation of the dicarbonyl complexes. An η^2-CO transition state of the type proposed for biscyclopentadienyl complexes of group 4 metals may be involved in the present insertion reaction. Similar bands were found for OTiCCO at 2047.7 and 976.5 cm^{-1} in titanium experiments.[31] The OMCCO molecules (M = Ti, Zr, Hf) are formed by near ultraviolet photochemical rearrangement of the $M(CO)_2$ dicarbonyls, reaction 5, which are calculated to be exothermic. These metals have a high density of allowed transitions in the ultraviolet region[29] for excitation of the metal in the dicarbonyl complexes.

$$M(CO)_2 \xrightarrow{\text{near ultraviolet}} OMCCO \qquad (M = Ti, Zr, Hf) \quad (5)$$

Part of the driving force for this reaction is oxidation of the metal from a M(0) to a M(II) complex involving the stable monoxide. We note that hydrolysis of the OMCCO species produced here would likely lead to the $C_2O_2^{2-}$ anion formed by electrochemical reduction of CO.[32]

The photochemical rearrangement to give the inserted OMCCO molecule has been observed for Nb, Ta, Th, and U as well as the group IV metals Ti, Zr, and Hf. The simple inserted carbide-oxide CMO molecule has been observed as a reaction product only for the actinides where the MCO → CMO rearrangement reaction is calculated to be exothermic.[15,16] However, in the case of NbCO, photochemical rearrangement of NbCO gave CNbO, which was computed to be 20 kcal/mol higher in energy.[14] In the present Zr and Hf cases, the CZrO and CHfO molecules are calculated to be 30 kcal/mol higher than the monocarbonyls, and these rearranged molecules are not observed here.

$M(CO)_2^-$. Weak bands at 1747.4 and 1681.0 cm^{-1} on sample deposition decreased together on annealing, disappeared on photolysis, and failed to reproduce on further higher temperature annealing. Both bands were reduced to less than 20% of the former yield with added CCl_4, which effectively traps laser-ablated electrons, so anion products must be considered.[26−28] In the mixed $^{12}C^{16}O + {}^{13}C^{16}O$ experiment, triplets with approximately 1:2:1 relative intensities were observed for both bands, indicating that two equivalent CO submolecules are involved in both modes. These two bands are assigned to the symmetric and antisymmetric C−O stretching vibrations of the bent $Hf(CO)_2^-$ anion. Our DFT calculation predicts a $^4B_2$ ground state for $Hf(CO)_2^-$ anion, with symmetric and antisymmetric C−O stretching vibrational frequencies at 1751.5 and 1727.5 cm^{-1} and 1689:769 relative intensities, which are in accord with the observed values.

Similar bands at 1745.9 and 1682.2 cm^{-1} in the Zr + CO experiments decreased together on annealing, disappeared on photolysis, and reduced to less than 20% of former yield with added CCl_4. These observations suggest an anion assignment. Both bands exhibited triplet isotopic structure in the mixed $^{12}C^{16}O + {}^{13}C^{16}O$ spectra. Our DFT calculation predicts a $^4B_2$ ground state for the $Zr(CO)_2^-$ anion with symmetric and antisymmetric C−O stretching vibrations at 1765.1 and 1712.7 cm^{-1} with 1385/1123 relative intensities, which confirms the $Zr(CO)_2^-$ anion assignment.

Our DFT calculation found a $^4\Delta$ ground state for the $ZrCO^-$ anion with C−O stretching vibration at 1767.1 (BP86) and 1815.9 (B3LYP) and for $HfCO^-$ $^4\Delta$ and $^2\Pi$ states very close in energy. The C−O stretching vibrational frequency was calculated at 1673.2 cm^{-1} for the $^2\Pi$ state and at 1766.9 cm^{-1} for the $^4\Delta$ state using the B3LYP functional. No obvious $ZrCO^-$ and $HfCO^-$ anion absorptions are observed in our experiments. The $Zr(CO)_2^-$ and $Hf(CO)_2^-$ anions appear to be formed by electron capture of the neutral molecules, which are exothermic reactions.

$$M(CO)_2 + e^- \rightarrow M(CO)_2^- \qquad (M = Ti, Zr, Hf) \quad (6)$$

The $Hf(CO)_2^-$ and $Zr(CO)_2^-$ anions are more stable by 48 and 38 kcal/mol than the neutral dicarbonyls, and these BP86/

(31) Zhou, M. F.; Andrews, L. *J. Phys. Chem. A* **1999**, *103*, 5259. The Ti/CO spectra were reexamined for product absorptions that appear on full-arc photolysis, and new bands were found at 2047.7, 976.5 cm^{-1} with $^{12}C^{16}O$ and at 2023.6, 935.6 cm^{-1} with $^{12}C^{18}O$.

(32) Uribe, F. A.; Sharp, P. R.; Bard, A. J. *J. Electroanal. Chem. Interfacial Electrochem.* **1983**, *152*, 173.

Table 9. Comparison of Observed C−O Stretching Vibrational Frequencies (cm^{-1}) for Group 4 Transition Metal and Th Carbonyl Species $M(CO)_x$ ($x = 1-3$)

	$x = 1$	$x = 2$	$x = 3$
Ti	1920.0	1893.1	1975.1
		1799.3	1840.3
Zr	1899.5	1855.5	1960.3
		1785.1	1838.2
Hf	1868.6	1850.9	1951.2
		1806.7	1835.5
Th	1817.5	1827.7	1919.2
		1775.6	1803.8

6-31+G(d) calculations provide an estimate of electron affinities until proper gas-phase measurements can be made. A slightly smaller electron affinity estimate was calculated for $Ti(CO)_2$ (35 kcal/mol),[31] and similar values were found for $Ru(CO)_2$ and $Os(CO)_2$.[33]

Other Absorptions. Several bands in both Zr and Hf reaction systems increased on higher temperature annealing. These may arise from species that contain more than one metal atom, and are simply labeled $M_x(CO)_y$ in the tables.

Bonding Considerations. Table 9 contrasts the C−O stretching vibrational frequencies of the group 4 transition metal and Th carbonyl species.[16,31] It is interesting to note that the C−O stretching frequencies for mono-, di-, and tricarbonyls *decreased* from Ti to Th, which indicates an *increase* in metal-to-carbonyl back-bonding in these series. Taking the monocarbonyl complexes as an example, TiCO is predicted to have a $^5\Delta$ ground state, which correlates with $s^1d^3(^5F)$ excited-state Ti 0.78 eV higher than the ^3F ground-state atom.[31,34,35] However, ZrCO, HfCO, and ThCO are predicted to have $^3\Sigma^-$ ground states, which reflect the s^2d^2 ground electron configuration of the metal atoms. All of these carbonyl complexes have four metal-based electrons in their valence electronic structure. For ZrCO, HfCO, and ThCO, there are two metal-based electrons occupying the σ molecular orbital, which are largely metal s in character and nonbonding, while for Ti, two metal-based electrons occupy one σ and one δ molecular orbital, respectively, and the δ orbital is mainly Ti 3d in character. The remaining two electrons occupy the doubly degenerate π molecular orbitals, which support significant metal d electron to CO π^* back-bonding and decrease in the C−O stretching frequency.

The decrease in MCO carbonyl frequencies going down the Ti family is also found for the early transition metal V and Cr families[31,36] but the *reverse* relationship is observed for the late transition metal Fe, Co, and Ni families.[28,31,33,36−38] These bonding trends are described by density functional calculations.

Table 10. Scale Factors (Observed/Calculated Frequencies) for Zr and Hf Carbonyls Using the BP86 Functional, the ECP+DZ for Zr and Hf, and the 6-31+G(d) Basis Set for C and O

carbonyl	Zr	Hf[a]
MCO	1.012	1.002
$M(CO)_2$	1.008[b]	1.012[b]
	0.983[c]	0.991[c]
$M(CO)_3$	1.010[b]	1.019[b]
	0.993[c]	0.994[c]
$M(CO)_4$	1.011[c]	1.012[c]
$M(CO)_2^-$	0.982[b]	0.998[b]
	0.982[c]	0.973[c]

[a] Calculations for $Hf(CO)_{2-4}$ employed D95* on C and O. [b] Symmetric C−O mode. [c] Antisymmetric C−O mode.

Conclusion

Laser-ablated zirconium and hafnium atoms have been reacted with CO molecules during condensation in excess neon. The $Zr(CO)_x$ and $Hf(CO)_x$ ($x = 1-6$) carbonyls were formed during sample deposition or on annealing. The OZrCCO and OHfCCO molecules were also formed by ultraviolet photochemical rearrangement of the $Zr(CO)_2$ and $Hf(CO)_2$ dicarbonyls, which provides a mechanism for CO activation by bonding to heavy metals. Evidence is also presented for the $Zr(CO)_2^-$ and $Hf(CO)_2^-$ anions. The decrease in carbonyl frequencies in the series TiCO, ZrCO, and HfCO is the reverse found for late transition metal families such as NiCO, PdCO,and PtCO,[38] and both trends are well-modeled by density functional theory.

Density functional theory calculations using core potentials for Zr and Hf atoms have been employed to help identify these products. The calculated C−O stretching vibrational frequencies and isotopic frequency ratios are in good agreement with observed experimental values. As can be seen from the scale factors listed in Table 10, which are in accord with other systems,[28,33,37−39] the BP86 functional *predicts the experimental frequencies within 1−2%*. Such predictive power is extremely useful. The match of observed and calculated isotopic ratios extends the agreement between experiment and theory from frequency positions to normal mode descriptions.

Acknowledgment. We gratefully acknowledge N.S.F. support for this research under Grant CHE 97-00116, helpful correspondence with C. W. Bauschlicher, several calculations done by B. Liang, and preliminary experiments performed by G. V. Chertihin.

JA9935613

(33) Zhou, M. F.; Andrews, L *J. Phys. Chem. A* **1999**, *103*, 6956 (RuCO).
(34) Fournier, R. *J. Chem. Phys.* **1993**, *99*, 1801.
(35) Adamo, C.; Lelj, F. *J. Chem. Phys.* **1995**, *103*, 10605.
(36) Zhou, M. F.; Andrews, L., work in progress (CrCO).
(37) Zhou, M. F.; Andrews, L *J. Phys. Chem. A* **1999**, *103*, 7773. (RhCO).
(38) Liang, B.; Zhou, M. F.; Andrews, L. *J. Phys. Chem. A*, in press (NiCO).
(39) Bytheway, I.; Wong, M. W. *Chem. Phys. Lett.* **1998**, *282*, 219.